Mechanism of Low Temperature ALD of Al_2O_3 on Graphene Terraces

Iljo Kwak[a,b], Jun Hong Park[a,b], Larry Grissom[c], Bernd Fruhberger[c], Andrew C, Kummel[b]

[a] Materials Science and Engineering Program, University of California, San Diego
[b] Department of Chemistry and Biochemistry, University of California, San Diego
[c] California Institute for Telecommunications and Information Technology, University of California San Diego

Uniform and defect-free Al_2O_3 films were grown on highly oriented pyrolytic graphite (HOPG) terraces by thermal atomic layer deposition (ALD) at low temperature (50 ^{o}C) without any functionalization of the surface. Controlling the pulse times of trimethylaluminum (TMA) and H_2O while using short Ar purge times, 1-2 nanometer size Al_2O_3 particles were formed on the HOPG terraces. The particles provided a layer of nanoscale nucleation centers on the HOPG terraces. Capacitance-voltage measurements of Al_2O_3 films grown at 50 ^{o}C using 50 ALD cycles showed an areal capacitance 1.17 $\mu F/cm^2$ with very small frequency dispersion, consistent with the absence of induction cycles and formation of a high quality interface. The leakage current of the Al_2O_3 was ~10^{-5} A/cm^2 in large area devices (1900 μm^2) which is comparable with results from devices prepared using an identical ALD process for Al_2O_3 on $Si_{0.7}Ge_{0.3}$(001) substrates, and is consistent with the absence of pinholes.

Introduction

Since its emergence in 2004 (1,2), single layer graphene has attracted attention due to its high mobility of charge carriers and charge confinement. Graphene has been viewed as a viable alternative channel material for future logic transistors because transistors based on silicon are approaching their fundamental limits.(3,4) However, in order to fabricate graphene devices, deposition of ultrathin, pinhole-free high-k dielectric gates is required. Atomic layer deposition (ALD) is the most effective method to deposit ultrathin high-k dielectric layers, due to excellent thickness control.(5) However, because of the inert nature of graphene surfaces, similar to the surfaces of carbon nanotubes (CNTs), conventional ALD dielectric layers selectively nucleate on defect sites or step edges.(6,7) In the conventional ALD process on graphene, such non-uniform oxides result in large leakage currents in devices.(8)

For CNTs, Farmer et functionalized the surface of CNTs using nitrogen dioxide (NO_2) and trimethylaluminum (TMA) at 25 ^{o}C to form an Al_2O_3 layer by ALD; however, the induction period for onset of uniform film growth was 100 ALD cycles.(9) Similarly,

several methods have been used to functionalize graphene surfaces including chemical treatment, deposition of oxidizing metal films, and polymer based seeding layers.(10, 11, 12, 13) Unfortunately, these functionalization methods can result in degradation of the electronic properties of graphene or require thick dielectric layers. Therefore, for successful fabrication of graphene devices, improved techniques for deposition of uniform and insulating gate oxides continue to be needed.

In this work, Al_2O_3 was directly deposited on highly oriented pyrolytic graphite (HOPG) surfaces by low temperature thermal ALD using TMA and H_2O without any seeding layer or surface treatments prior to deposition. With the substrates at a temperature of 50 ^oC, using short purge times between the two precursor pulses and long pulses of the precursors, a CVD growth component was intentionally employed to provide more nucleation sites on the surface. The CVD growth component induces formation of 1-2 nanometer Al_2O_3 particles on the surface which provide nucleation centers for uniform deposition. The deposited Al_2O_3 film was continuous and uniform without observable defects. The surface morphology of the oxide was analyzed by atomic force microscopy (AFM) and electrical properties were characterized by capacitance-voltage and leakage current measurements of metal/Al_2O_3/HOPG stacks.

Experimental Techniques

HOPG samples (from SPI supplies) were cleaned by the mechanical exfoliation method using an adhesive tape. The samples were loaded into a commercial ALD reactor (Beneq TFS 200 ALD system) which has a hot wall, crossflow reaction chamber. The reaction chamber was pumped down to 1 mTorr. To deposit Al_2O_3, TMA and H_2O were used as ALD precursors, temperature stabilized at 20 ^oC. The carrier gas was research purity argon (Ar, Praxair, 99.9999%) which was flowed at 300 sccm (standard cubic centimeter). 50 cycles of ALD were employed, each cycle consisting of a sequence of 600 ms TMA pulse, 500 ms Ar purge, 50 ms H_2O pulse, and 500 ms Ar purge. For comparison, using identical ALD pulse times, films were grown with sample temperatures between 50 ^oC to 200 ^oC to investigate the effect of temperature on the nucleation of Al_2O_3. To compare nucleation behavior on a highly reactive substrate, Al_2O_3 was deposited on $Si_{0.7}Ge_{0.3}$(001) substrates using 50 cycles of ALD, consisting of sequences of 300 ms or 400 ms TMA pulses followed by 50 ms H_2O pulses with 500 ms Ar purge at 50 ^oC sample temperature. In addition, the effect of the precursor pulse times on the morphology of the oxide on HOPG were studied. TMA and H_2O pulse durations were changed from 200 ms to 600 ms and 50 ms to 150 ms, respectively, while the sample temperature during ALD was fixed at 50 ^oC.

After the ALD process, non-contact mode AFM measurements were performed to determine the correlation between the surface topography and the ALD conditions. MIM (Metal-Insulator-Metal) capacitors were fabricated to characterize the electrical properties of the oxide. In order to compare the quality of the oxide, $Si_{0.7}Ge_{0.3}$ substrates were loaded along with the HOPG samples. Al_2O_3 was deposited on HOPG and $Si_{0.7}Ge_{0.3}$(001) using 50 cycles of ALD with the samples at 50 ^oC. After the ALD process, Ni gates were deposited on the oxide by thermal evaporation. The gates were 50 μm in diameter and 3 nm thick. As a control, Ni/Al_2O_3/$Si_{0.7}Ge_{0.3}$/Al metal–oxide–

semiconductor capacitors (MOSCAPs) were also fabricated with a slightly different process due to different cleaning and contact requirements. Prior to ALD, each $Si_{0.7}Ge_{0.3}$(001) sample was treated with a 30 s rinse by each of acetone, isopropyl alcohol, and DI water followed by N_2 drying. Afterwards, the native oxide was removed by cyclic HF cleaning using a 2% HF solution and DI water at 25 ^oC for 1 min in each solution for 2.5 cycles.(14) For each SiGe sample, 50 cycles of ALD deposition were followed by Ni gate deposition and 100-nm thick Al back contact deposition using DC sputtering. For both the HOPG and SiGe samples, the capacitance-voltage curves were measured in the frequency range of 2 kHz to 1MHz at room temperature with an HP4284A LCR meter. Leakage current of current of the oxide was obtained in the range of -2V to 2V.

Results and Discussion

Temperature dependence of Al_2O_3 ALD

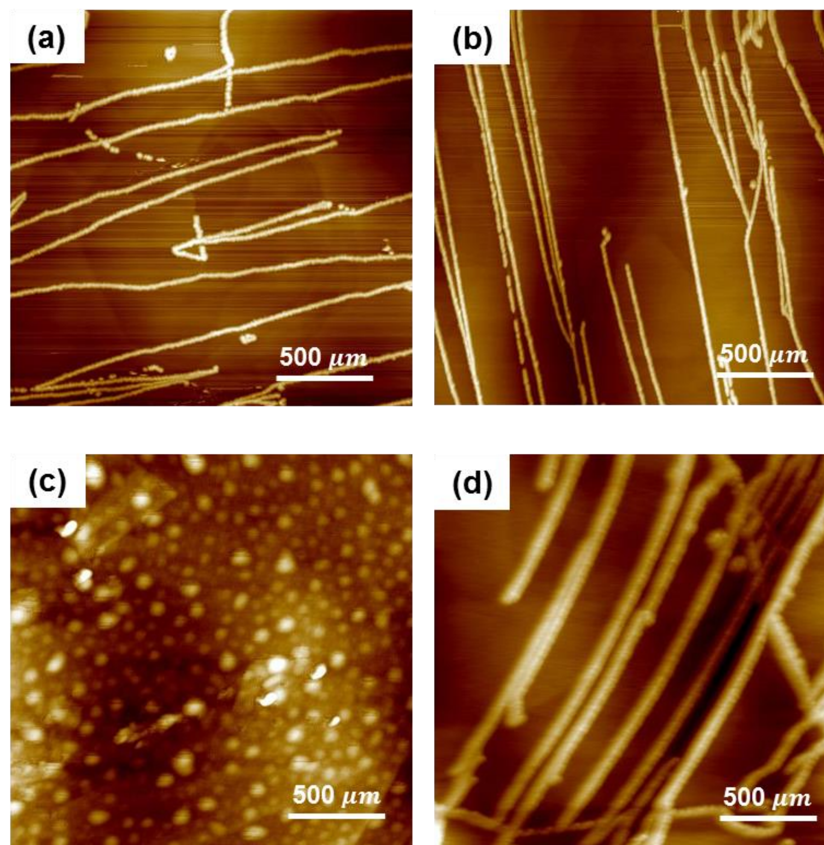

Figure 1. (Color) AFM images of Al_2O_3 films (50 ALD cycles) on HOPG with different sample growth temperatures. (a) 200 ^oC, (b) 150 ^oC and (c) 50 ^oC. Each ALD cycle consisted of a 600 ms TMA pulse, 500 ms Ar purge, 50 ms H_2O pulse, and 500 ms Ar purge. (d) 50 ALD cycles of Al_2O_3 were deposited with 2 s purge times at sample termperature of 50 ^oC, using otherwise identical ALD conditions as for the samples in (a), (b), (c). Non-contact mode AFM measurements were carried out with a Si tip. Note that for high temperature ALD, the nucleation of Al_2O_3 was only observed along the step edges while for low temperature ALD, the nucleation was observed across the terraces and the step edges. In addition, for low temperature ALD, 1-2nm spheres were observed on the surface. The size of each image is 2x2 μm^2.

Figure 1 shows AFM images of Al_2O_3 grown on HOPG using 50 cycles of ALD at sample temperatures of 200 °C, 100 °C, and 50 °C. Each ALD cycle for the samples of Figs. 1(a),(b),(c) consisted of 600 ms TMA pulse and 50 ms H_2O pulse, with 500 ms Ar purge times between precursor pulses. The growth of Al_2O_3 exhibited strong dependence on sample temperature. As shown in Figs. 1 (a) and (b), when the sample temperature was above 100 °C, Al_2O_3 was only deposited on the step edges of the HOPG and not on the terraces, because dangling bonds for nucleation are only available on the step edges and not on the inert terraces. The thickness of the Al_2O_3 deposited on the step edges was about 5 nm which is consistent with the expected thickness for 50 cycles of ALD at the typical 0.1 nm/cycle ALD growth rate.(15)

When the sample temperature was decreased to 50 °C as shown in Fig. 1(c), the Al_2O_3 film was deposited continuously on both the step edges and the terraces without pin hole formation. Spherical Al_2O_3 features were observed across the entire surfaces for the growth at 50 °C sample temperature. However, these features are only observed with a short purge time between two precursor pulses at 50 °C sample temperature. When the purge time was increased to 2s with identical precursor ALD pulse times and sample temperature, the spherical Al_2O_3 features were not observed as shown in Fig 1(d). Short purge times can induce a chemical vapor deposition (CVD) growth component since excess unreacted physisorbed precursor molecules have insufficient time to desorb from both the substrate and chamber walls during the short purge time. The CVD component induced deposition of particles of about 2 ± 0.4 nm diameter which was quantified by averaging 10 AFM line scans. Al_2O_3 particles on the surface were formed by either nucleation in the ALD chamber and subsequently transported to the sample surface or were formed by precursor islands on the surface. Since surface island growth is usually non-spherical and similar nuclei were also observed on the reactive SiGe surface (Fig 2(a),(b)), the data is most consistent with nuclei formation in the ALD chamber (denoted gas phase nucleation below).(16, 17)

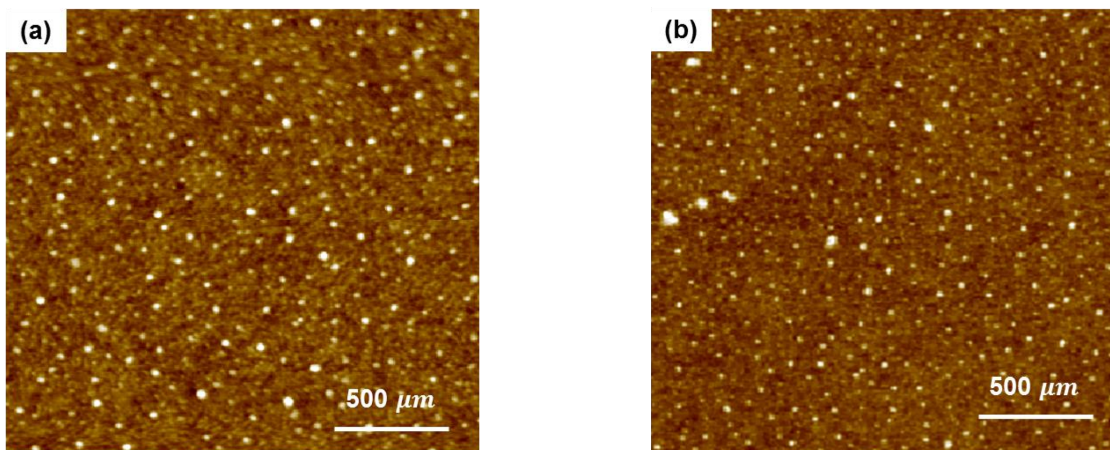

Figure 2. (Color) AFM images of Al_2O_3 films (50 ALD cycles) on $Si_{0.7}Ge_{0.3}$(001) grown at 50 °C sample temperature. ALD was carried out using sequences of (a) 300 ms TMA pulse and 50 ms H_2O pulse with 500 ms of Ar purge after each precursor pulse, (b) 400 ms TMA pulse and 50 ms H_2O pulse with 500 ms of Ar purge after each precursor pulse at 50 °C sample temperature. Spherical Al_2O_3 nuclei were observed on SiGe (white dots). This data is consistent with nuclei formation in the ALD chamber. The size of each image is 2x2 μm^2.

Effect of precursor pulse time on Al_2O_3 ALD

Figure 3 (a)-(c) shows the AFM images of Al_2O_3 grown by ALD at 50 ^oC sample temperature with different pulse lengths of TMA and H_2O with a fixed Ar purge time of 500 ms. For the sample with 200 ms TMA pulses and 50 ms H_2O pulses (Fig. 3(a)), Al_2O_3 was mainly deposited on the step edges. Although some Al_2O_3 was nucleated on the terraces, it was discontinuous with a high density of visible pinholes. The number densities of the Al_2O_3 particles (number of particles per 4 μm^2 image area) with the three different ALD conditions are shown in Table I. For the sample shown in Fig. 3(a), grown using relatively short 200 ms TMA pulses, the density of the Al_2O_3 particles ($15/\mu m^2$) was significantly lower than for the samples shown in Figs. 3(b),(c), which were grown under different conditions with longer TMA pulse times. When the TMA pulse time was increased to 600 ms while fixing the H_2O pulse length (Fig. 3(b)), the density of the Al_2O_3 particles was markedly increased ($123/\mu m^2$) and continuous Al_2O_3 films were deposited on both terraces and step edges without pinholes. AFM line traces show that the particles are 2 ± 0.6 nm in diameter (Fig 3(e)). The observation of the high density of defects and low density of Al_2O_3 particles in the dielectric deposited using short TMA pulses indicates that the Al_2O_3 particles have a critical role in the formation of uniform dielectric layers on HOPG during ALD.

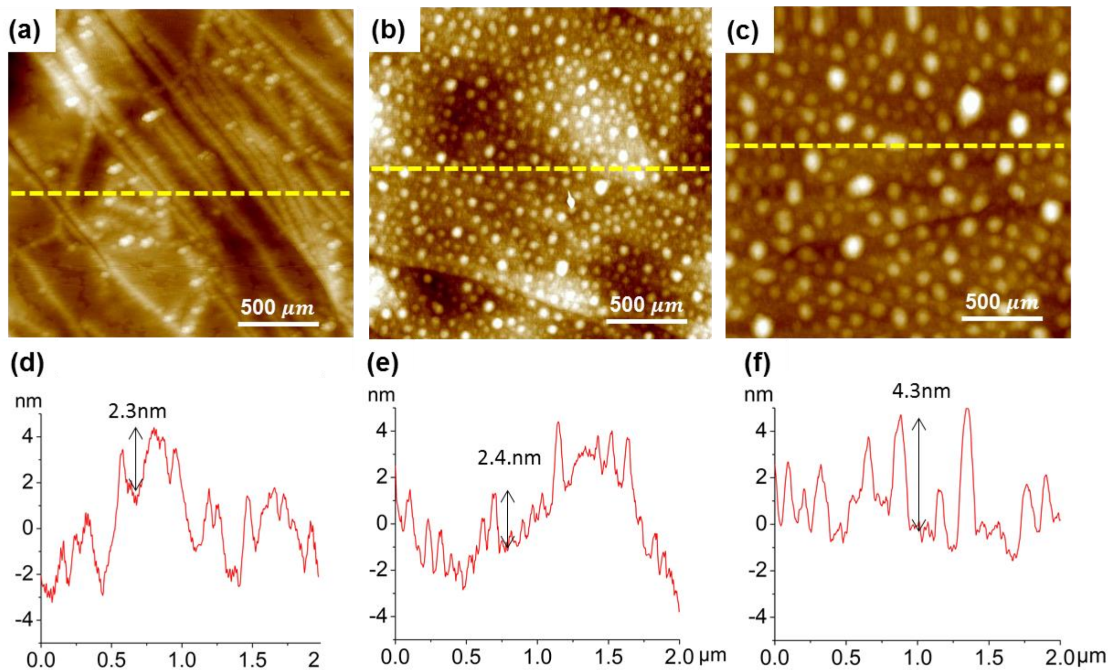

Figure 3. (Color) AFM images of Al_2O_3 films (50 ALD cycles) on HOPG (a) 200 ms TMA and 50 ms H_2O pulses, (b) 600 ms TMA and 50 ms H_2O pulses, and (c) 600 ms TMA and 150 ms H_2O pulses. (d), (e), and (f) are AFM height profiles along the yellow lines in Figs. (a), (b) and (c) respectively. For the ALD with short pulses ((a), (d)), few condensation nuclei were observed, and the ALD nucleation primarily occurred on the step edges. For the two samples grown with longer TMA pulses ((b), (e) and (c), (f)), white condensation nuclei were distributed across the terraces, and ALD nucleation occurred on both the terraces and the step edges.

When the H_2O pulse time was increased to 150 ms with a fixed TMA pulse time of 200 ms (Fig. 3(c)), similar morphology as for the growth with a long TMA pulse (Fig. 3(b)) was observed. The Al_2O_3 film was continuous with a high density of Al_2O_3 particles (44/μm^2). AFM lines traces (Fig. 3(f)) show the particles increased in size to 4 ± 0.7 nm. This indicates that the Al_2O_3 particles were formed by a CVD component that can be controlled by the TMA and H_2O pulse times. This observation is consistent with both the island formation mechanism and the gas phase formation mechanism for the particles.

TABLE I. Number density of Al_2O_3 particles from films grown with different ALD conditions (Number of particles per 4 μm^2)

200 ms TMA & 50 ms H_2O pulses	600 ms TMA & 50 ms H_2O pulses	200 ms TMA & 150 ms H_2O pulses
59	692	176

Electrical Properties

MIM capacitors were fabricated on freshly cleaved HOPG substrates. Al_2O_3 films were deposited using 50 ALD cycles consisting of 600ms TMA pulse, 500 ms Ar purge, 50 ms H_2O pulse, and 500 ms Ar purge at 50 ^{o}C sample temperature. Subsequently, Ni metal gates were deposited by thermal evaporation. The area of the capacitor was ~1900 μm^2 (50 μm diameter). Capacitance-voltage (C-V) and leakage current-voltage (I-V) measurements were performed in order to evaluate the electrical quality of the oxide. As shown in Fig. 4(a), the capacitance of the oxide was nearly independent of the applied voltage owing to the MIM structure of the capacitor. Previously, Park et al reported fully modulated capacitance of Al_2O_3/monolayer TiOPc/graphene stacks.(18) For single layer graphene, capacitance can be modulated near 0 V due to the linear dispersion of the density of states near the Fermi energy level. However, because of the high charge carrier density of HOPG near the Fermi energy level, the modulation of capacitance was not observed. The C_{max} of the oxide was 1.17 $\mu F/cm^2$ which is consistent with the C_{max} value of the ALD grown Al_2O_3 on $Si_{0.7}Ge_{0.3}$(001) as shown in Fig. 4(b). This indicates that deposition of Al_2O_3 on HOPG proceeded without an ALD induction time. Note the high dispersion of the C-V data on $Si_{0.7}Ge_{0.3}$ was likely due to the formation of GeOx which can be suppressed by $(NH_4)_2S$(aq) or NH_3 plasma treatments.(19, 20) However, these cleaning recipes were not employed in this study since they may induce unintentional chemical changes of HOPG and degradation of the surface quality on HOPG.

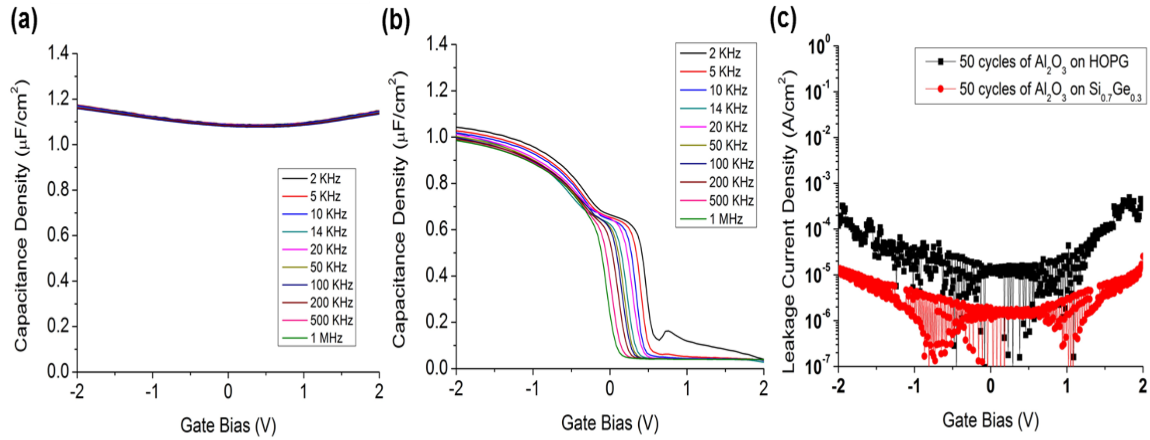

Figure 4. (Color) Comparison of Electrical Properties of Low Temperature Al_2O_3 ALD on HOPG and $Si_{0.7}Ge_{0.3}$(001) with cycles consisting of a 600 ms TMA pulse, 500 ms Ar purge, 50 ms H_2O pulse, and 500 ms Ar purge at 50 ^oC sample temperature.(a) Capacitance vs. Voltage Curve of Ni/Al_2O_3(50 ALD cycles)/HOPG stack. (b) Capacitance vs. Voltage Curve of Ni/ Al_2O_3(50 ALD cycles)/$Si_{0.7}Ge_{0.3}$/Al stack. (c) I-V curve of Ni/ Al_2O_3(50 ALD cycles)/HOPG and Ni/ Al_2O_3(50 ALD cycles)/$Si_{0.7}Ge_{0.3}$/Al stack. The similar Cox on HOGP and $Si_{0.7}Ge_{0.3}$(001) is consistent with no ALD induction cycles on HOPG. The comparable leakage currents of Al_2O_3/HOPG to Al_2O_3/$Si_{0.7}Ge_{0.3}$ are consistent with the oxide on HOPG being uniform and pin-hole free on the HOPG substrate.

Figure 4 (c) compares the leakage currents of Al_2O_3 films grown by 50 ALD cycles on HOPG (red) and $Si_{0.7}Ge_{0.3}$(001) (blue) substrates. ALD was performed simultaneously at 50 ^oC sample temperature on the two substrates. The leakage current of the oxide on the HOPG was 3.1×10^{-5} A/cm^2 and 2.2×10^{-6} A/cm^2 for the $Si_{0.7}Ge_{0.3}$ at -1 V. The low leakage on $Si_{0.7}Ge_{0.3}$ is expected since Al_2O_3 readily nucleates on $Si_{0.7}Ge_{0.3}$(001), and the $Si_{0.7}Ge_{0.3}$(001) surface is flat without bunched steps. Conversely, HOPG surfaces are inert and have bunched steps.(16, 18) The leakage current of the ALD grown Al_2O_3 on HOPG at 50 ^oC sample temperature being within 15x of the leakage current on $Si_{0.7}Ge_{0.3}$(001) is consistent with the oxide on HOPG being uniform and pin-hole free on the HOPG substrate.

Conclusion

Deposition of high quality Al_2O_3 films on HOPG was demonstrated by low temperature ALD without evidence for an ALD induction period prior to onset of uniform film growth. Controlling the pulse times of TMA and H_2O along with a short purge time, 1-2 nanometer diameter spherical Al_2O_3 particles were formed on both HOPG and SiGe consistent with a gas phase reaction of the ALD precursors. The nuclei provided uniform nucleation centers on the inert HOPG surface resulting in uniform and pin-hole free Al_2O_3 films on both step edges and terraces. Comparable C_{ox} for low temperature ALD grown Al_2O_3 on HOPG and $Si_{0.7}Ge_{0.3}$(001) is consistent with the absence of induction cycles even on the inert HOPG surface. The leakage current of the Al_2O_3 was as low ~10^{-5} A/cm^2 which is within 15x of the leakage current observed for

Al_2O_3 on highly recative $Si_{0.7}Ge_{0.3}(001)$ substrates. This work has great potential for fabrication of novel graphene-based devices.

Acknowledgments

This work is supported in part by the National Science Foundation Grant DMR 1207213, by the Center for Low Energy Systems Technology (LEAST), a STARnet Semiconductor Research Corporation (SRC) program sponsored by MARCO and DARPA, and by the SRC Nanoelectronic Research initiated through the South West Academy of Nanoelecronics (SWAN). Experiments were performed in the UCSD Nano3 facility supported by the NNCI (ECCS-1542148).

References

1. K. S. Novoselov, A. K. Geim, S. V. Morozov, D. Jiang, Y. Jiang, S. V. Dubonos, I. V. Grigirieva, and A. A. Firsov, Science, 306, 666 (2004).
2. K. S. Novoselov, A. K. Geim, S. V. Morozov, D. Jiang, M. I. Katsnelson, I. V. Grigorieva, S. V. Dubonos, and A. A. Firsov, Nature (London), 438, 197 (2005).
3. D. Alamo, J. A. Nature 479.7373 (2011).
4. Y. Xuan, Y.Q. Wu, P. D. Ye, Electron Device Letters, IEEE 29.4 (2008)
5. R.L. Puurunen, J. Appl. Phys. 97, 121301 (2005)
6. Y. Xuan1, Y. Q. Wu1, T. Shen1, M. Qi1, M. A. Capano1, J. A. Cooper1 and P. D. Ye, Birck and NCN Publications (2008)
7. X Wang, SM Tabakman and H Dai,,Journal of the American Chemical Society 130.26 (2008)
8. W. Y. Fu, L. Liu, W.L. Wang, M. H. Wu, Z. Xu, X. D. Bai and E. G. Wang, Science China Physics, Mechanics and Astronomy 53, no. 5 (2010)
9. D. B. Farmer, and R. G. Gordon, Nano letters 6, no.4 (2006)
10. M. J. Hollander, M. LaBella, Z. R. Hughes, M. Zhu, K. A. Trumbull, R. Cavalero, D. W. Snyder, X. Wang, E, Hwang, S. Datta, and J. A. Robinson, Nano letters 11. No. 9 (2011)
11. B. Fallahazad, B., K. Lee, G. Lian, S. Kim, C. M. Corbet, D. A. Ferrer, L. Colombo, and E. Tutuc, Applied Physics Letters 100, no. 9 (2012)
12. S. S. Tinchev, Applied Surface Science 258.7 (2012)
13. B. Lee, S. Y. Park, H. C. Kim, K. J. Cho, E. M. Vogel, M. J. Kim, R. M. Wallace, and J. Kim, Applied Physics Letters 92, no. 20 (2008)
14. O. Yasuhiro, M. Shandalov, Y. Sun, P. Pianetta, and P. C. McIntyre. Applied Physics Letters 94, no. 18 (2009)
15. Y, Kim, S. M. Lee, C.S. Park, S.I. Lee, M.Y. Lee, Applied Physics Letters 71 (1997): 3604-3606.
16. M. Volmer and A. Weber, Z. phys. Chem 119.3/4 (1926)
17. M. Volmer and A. Weber. Nucleation in super-saturated products (1988).
18. J.H. Park, H. C. Movva, E. Chagarov, K. Sardashti, H. Chou, I. Kwak, K. T. Hu, S. K. Fullerton-Shirey, P. Choudhury, S. K. Banerjee, A. C. Kummel, Nano letters 15, no. 10 (2015)

19. K. Sardashti K, K. T. Hu, K. Tang, S. Park, H. Kim, S. Madisetti, P. McIntyre, S. Oktyabrsky, S. Siddiqui, B. Sahu, N. Yoshida, J. Kachian and A. C. Kummel, Interfaces. Applied Surface Science. (2016)
20. K. Sardashti, K. T. Hu, K. Tang, S. Madisetti, P. McIntyre, S. Oktyabrsky, S. Siddiqui, B. Sahu, N, Yoshida, J. Kachian, B. Fruhberger and A. C. Kummel, Applied Physics Letters 108, no. 1 (2016)